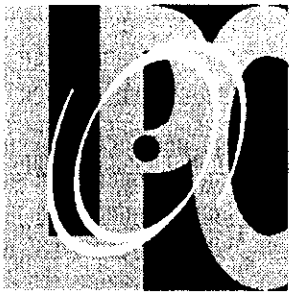

Laboratoire de Physique Corpusculaire
de Clermont-Ferrand

Deeply Virtual Compton Scattering at 11 GeV

P.Y. BERTIN, Y. ROBLIN

Laboratoire de Physique Corpusculaire de Clermont-Ferrand,
IN2P3/CNRS - Université Blaise Pascal,
F-63177 Aubière, France

C.E. HYDE-WRIGHT, F. SABATIE

Old Dominion University, Norfolk,
Virginia 23508 – U.S.A.

Deeply Virtual Compton Scattering At 11GeV

P.Y. BERTIN and Y. ROBLIN
IN2P3/CNRS and Université Blaise Pascal, Clermont-Ferrand, FRANCE
C.E. HYDE-WRIGHT and F. SABATIE
Old Dominion University, Norfolk, USA

(June 22, 2000)

1 Introduction

The understanding of the structure of the nucleon is a fundamental topic. Despite having been studied during the past forty years, there are still many questions left unanswered. An example of such is the extensive debate over the spin structure of the nucleon ground state. Two kinds of observables linked to the nucleon structure have been considered so far. Electromagnetic form factors, first measured on the proton by Hoftstader [1] in the 1950's, then more recently on the neutron [2]. Weak form factors have been measured in parity violating experiments [3]. Another approach initiated in the late 60's [4] studies parton distribution functions via Deep Inelastic Scattering (DIS)[5], [6] and Drell-Yan processes [7].

Recently a new theoretical framework has been proposed, namely the Skewed Parton Distributions (SPD). They provide an intimate connection between the ordinary parton distributions and the elastic form factors and therefore contain a wealth of information on the quark-gluon structure of the nucleon.

The QCD factorization theorems [8, 9] have established that the SPD's can be measured via exclusive reactions in the so-called deep virtual limit (fixed Bjorken variable x_B, $Q^2 >> \Lambda^2_{QCD}$, $Q^2 >> -t$, $t = (p' - p)^2$, where p and p' correspond to the initial and recoil proton four-vectors respectively). These deep virtual processes include $ep \rightarrow ep\pi^0$, $ep \rightarrow en\pi^+$, $ep \rightarrow eN^*\gamma$ and $ep \rightarrow ep\gamma$, ... Of course, the connection between the SPD's and the deep virtual measurements is subject to the same kind of higher twist corrections as in the case of ordinary parton distributions and deep inelastic scattering.

The simplest exclusive process to study that can be described in terms of SPD's is the Deeply Virtual Compton Scattering (DVCS) , $ep \rightarrow ep\gamma$.

We propose intensive measurement of the Deeply Virtual Compton Scattering process $ep \rightarrow ep\gamma$ at Jefferson Lab with a beam energy up to 11 GeV. First we will be able to explore the onset of Q^2 scaling, by measuring a beam helicity or charge asymmetry for Q^2 ranging from 0.5 to 5 GeV^2 and a x_B range in the valence region, from 0.2 to 0.5. At this kinematics, the asymmetries are dominated by the DVCS - Bethe-Heitler (BH) interference. The beam helicity asymmetry turns out to be proportional to the imaginary part of the DVCS amplitude amplified by the full BH amplitude, whereas the charge asymmetry is proportionnal to the real part of the DVCS amplitude with the same BH amplification.

One can expect to observe an early scaling of the DVCS amplitude. Indeed, the imaginary part of the forward Compton amplitude measured in deep inelastic scattering (via the optical theorem) scales at Q^2 as low as 1 GeV^2. If the scaling is reached, the measurement of the asymmetries would allow us to access the skewed parton distributions (SPD) contributing to the DVCS amplitude.

We want to emphasize that it is not one experiment that we want to propose, but a consistent research program that will allow us to access correlations of quarks inside the nuclear matter. This program must take advantage of the high intensity polarized electron beam available at Jefferson Lab, allowing to work at luminosities as high as 10^{37} /nucleon/cm^2/s with magnetic spectrometers that exist or to be upgraded in the Hall A or C. This luminosity is 10^5 to 10^6 larger than what is available at competitive facilities like HERMES or COMPASS in their best condition.

In addition, Hall B with its large acceptance spectrometer CLAS is the best place to develop a program using a positron beam. Hall B is well suited to accomodate ~ 10 nA beam corresponding to a luminosity of $5 \cdot 10^{34}$. A positron beam of 10 nA is the limit at which CLAS can operate, and is somewhat straightforward to achieve with a limited investment. Using CLAS in Hall B, a full program would allow various checks of SPD models through the knowledge of the full DVCS amplitude (both the imaginary and the real part). In addition, Hall A and C at lower luminosities (10^{36}) as well as Hall B could perform polarized target experiments (polarized NH_3 for instance).

2 Theory

The DVCS reaction $\gamma^* p \rightarrow \gamma p$ has become a subject of considerable new interest. This process can be measured in the exclusive electroproduction reaction $ep \rightarrow ep\gamma$ in deep inelastic scattering kinematics. Recently X. Ji [10], [11] suggested using DVCS to get information about a new class of parton distribution functions, which he called Off-Forward Parton Distributions (OFPD). These parton functions generalize the concept of the parton distributions found in DIS (Fig. 1). They describe off-diagonal matrix elements and can be interpreted as quark correlation functions, unlike the usual parton distributions which represent probabilities.

These OFPD's, also known as Skewed Parton Distributions (SPD) contain a wealth of information on the spin structure of the proton. In particular, it has been shown that there is a sum rule relating the SPD's to the total angular momentum (spin and orbital) carried by the quarks [10].

The DVCS amplitude can be factorized in a soft part containing the non-perturbative physics and described by the SPD's and a parton process, calculable via perturbative QCD (pQCD) [8, 9, 12]. This is depicted in Fig. 1b and because of its topology, is commonly called the handbag diagram. It exhibits a Bjorken type Q^2 scaling behavior at fixed $x_B = Q^2/(2p.q)$ and fixed invariant momentum transfer between the initial and scattered proton. It has been demonstrated that the QCD Q^2 evolution equations of the SPD's combine the Dokshitser-Gribov-Lipatov-Altarelli-Parisi (DGLAP) evolution [13] of usual parton distributions and the Efremov-Radyushkin-Brodsky-Lepage (ERBL) evolution [14] of meson distribution amplitudes in contrast with the DIS case where only DGLAP occurs [11]. The radiative corrections to the handbag diagram in DVCS have been evaluated up to next-to-leading order [15] in α_s.

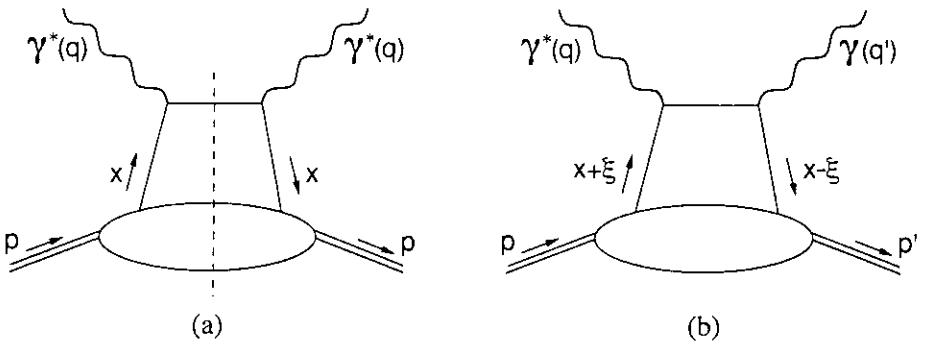

Figure 1: (a) Forward virtual Compton amplitude which describes the DIS cross-section via the optical theorem ($x_B = x$); (b) Handbag diagram occurring in the DVCS amplitude ($x_B = 2\xi/(\xi + 1)$ at the deep virtual limit).

The deep inelastic scattering cross section is related to the forward Compton amplitude via the optical theorem. In the limit of DIS, this forward amplitude is dominated by the handbag diagram of Fig. 1a. On the other hand, the off-forward Compton amplitude of Fig. 1b directly describes the DVCS amplitude in the deeply virtual limit of large Q^2, large $s = (q + p)^2$ and small $t = (p' - p)^2$.

The momentum transfer to the proton $(p' - p)$ is characterized by two values: the invariant

momentum transfer squared t, and the + component of the light cone momentum fraction ξ[10][1]: $\xi = (p - p')^+/P^+$, where $P = (p + p')/2$.

The extra degrees of freedom given by the t and ξ variables are what makes the dynamics of DVCS so rich and diverse. Depending on the kinematical domain, the SPD's can represent either the correlation between two quarks of momentum fractions $x + \xi$ and $x - \xi$, two antiquarks or between a quark and an antiquark (see Fig. 3).

A unique feature of DVCS is that by exploiting the interference between the DVCS and the Bethe-Heitler process where the real photon is radiated by the lepton, and which is completely calculable, it is possible to measure the real and imaginary part of the DVCS amplitude independently (Fig. 2). This fact has been known for a long time [16].

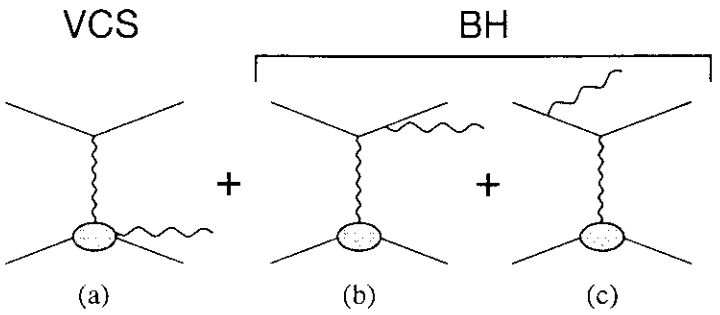

Figure 2: The DVCS process (a) along with the interfering Bethe-Heitler diagrams (b) and (c)

The helicity structure of DVCS is interesting in itself and gives rise to an angular dependence on the variable φ, the angle between the leptonic and hadronic planes. Diehl *et al.* [17] pointed out ways of using this structure to test the handbag diagram contribution to the DVCS amplitude.

The Q^2 at which the handbag dominance occurs can currently not be predicted from QCD. This is also true for DIS. At moderate Q^2, the higher twist corrections remain problematic in DIS as they are hard to disentangle from the leading term and its log behavior in Q^2. In the case of DVCS, we have the opportunity to gain detailed information on the size of these higher twists and determine the onset of scaling since each of the helicity amplitudes has a specific lowest twist.

There are two specific observables that we propose to measure:

- the cross section difference for leptons of opposite helicities. This observable is non-zero only if the detected photon is out of the electron scattering plane. This cross-section difference is proportional to the interference of the imaginary part of the DVCS amplitude with a known BH weight.

- the cross section difference for leptons of opposite charge. The asymmetry appears because the DVCS diagram has 1 coupling on the leptonic lines (virtual photon) and the BH has 2 such couplings (virtual photon and real photon). This cross-section difference is proportional to the interference of the real part of the DVCS amplitude with a known BH weight and has a characteristic angular dependence.

The $\gamma^* p \to \gamma p$ subprocess can be described by 12 helicity amplitudes, among which 2 cancel out. The angular dependence in φ allows us to access these helicity amplitudes, and in particular separate those which are leading twist from those which are not. This gives us an additional handle to observe the onset of scaling. In the regime where the factorization is valid it will then be possible to extract some of the SPD distributions.

[1]Other authors [12] use the alternate notation $\zeta = (p - p')^+/P^+$, but in this case, they refer to $P = p$.

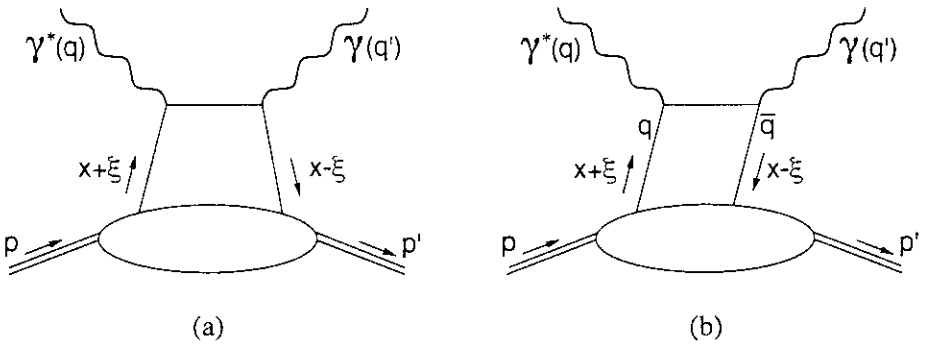

Figure 3: Dynamical behavior of the DVCS amplitude: a) q-q ($x+\xi$, $x-\xi > 0$) or $\bar{q}$-$\bar{q}$ ($x+\xi$, $x-\xi < 0$) distribution function; b) q-$\bar{q}$ correlation function ($x+\xi > 0$, $x-\xi < 0$). Unlike the DIS diagram of Fig. 1a, the DVCS amplitude also includes the crossed diagrams in which the virtual and real photons are exchanged.

3 DVCS cross section and asymmetry

3.1 DVCS cross-section and SPD models

The full DVCS cross section has been computed at the leading twist in $1/Q$ taking into account the interference with the Bethe-Heitler [18], using some models for the SPD functions. These SPD models obey a number of constraints such as positivity bounds and parity considerations. Nevertheless there is still considerable freedom in constructing such models and several have been published [18, 19, 20, 21, 22, 23]. Figure 4 shows the DVCS cross-section computed using models from reference [18].

The $ep \rightarrow ep\gamma$ cross-section is given by:

$$\frac{d^5\sigma^{lp\rightarrow lp\gamma}}{dQ^2 dx_B dt d\varphi} = \frac{\alpha_{em}^3}{8\pi} \frac{1}{4x_B M_p^2 E_{lab}^2} \frac{1}{\sqrt{1+4x_B^2 M_p^2/Q^2}} \left|\mathcal{T}_{BH} + \mathcal{T}_{VCS}\right|^2 \quad (1)$$

where $\mathcal{T}_{VCS}$ and $\mathcal{T}_{BH}$ are the amplitudes for the VCS and Bethe-Heitler processes, x_B is the Bjorken variable, φ is the angle between the hadronic and the leptonic planes, t is the transfer between the initial and final state proton defined by $t = (p' - p)^2$.

As we can see from Fig. 4, the Bethe-Heitler dominates the cross-section in energies accessible at Jefferson Lab. It would be very difficult to separate the DVCS cross-section from the Bethe-Heitler. However, as discussed in the previous section, we can benefit from the situation if we consider the difference in cross-section for electrons of opposite helicities or charge. There is no contribution coming from the $|BH|^2$ term. This term, being purely real does not contribute because of symmetry reasons [10]. In our kinematics, the $|DVCS|^2$ contribution is strongly suppressed and the term dominating this cross-section difference is the interference between the BH and the DVCS.

We will effectively use this interference with the BH as a filter and a magnifier. Indeed, it projects out either the imaginary part(helicity difference) or the real part(charge difference) of the DVCS amplitude and also enhances it with the full magnitude of the BH.

4 Experimental requirements

A complete discussion of the experimental apparatus along with a detailed simulation can be found in [24]. The deeply virtual Compton scattering at 6 GeV proposal [25] is submitted to PAC18 and is also a good source of information. All the information about the experimental background issues of associated production or direct π^0 production, which are the main difficulties of this experiment are adequately discussed in those two references.

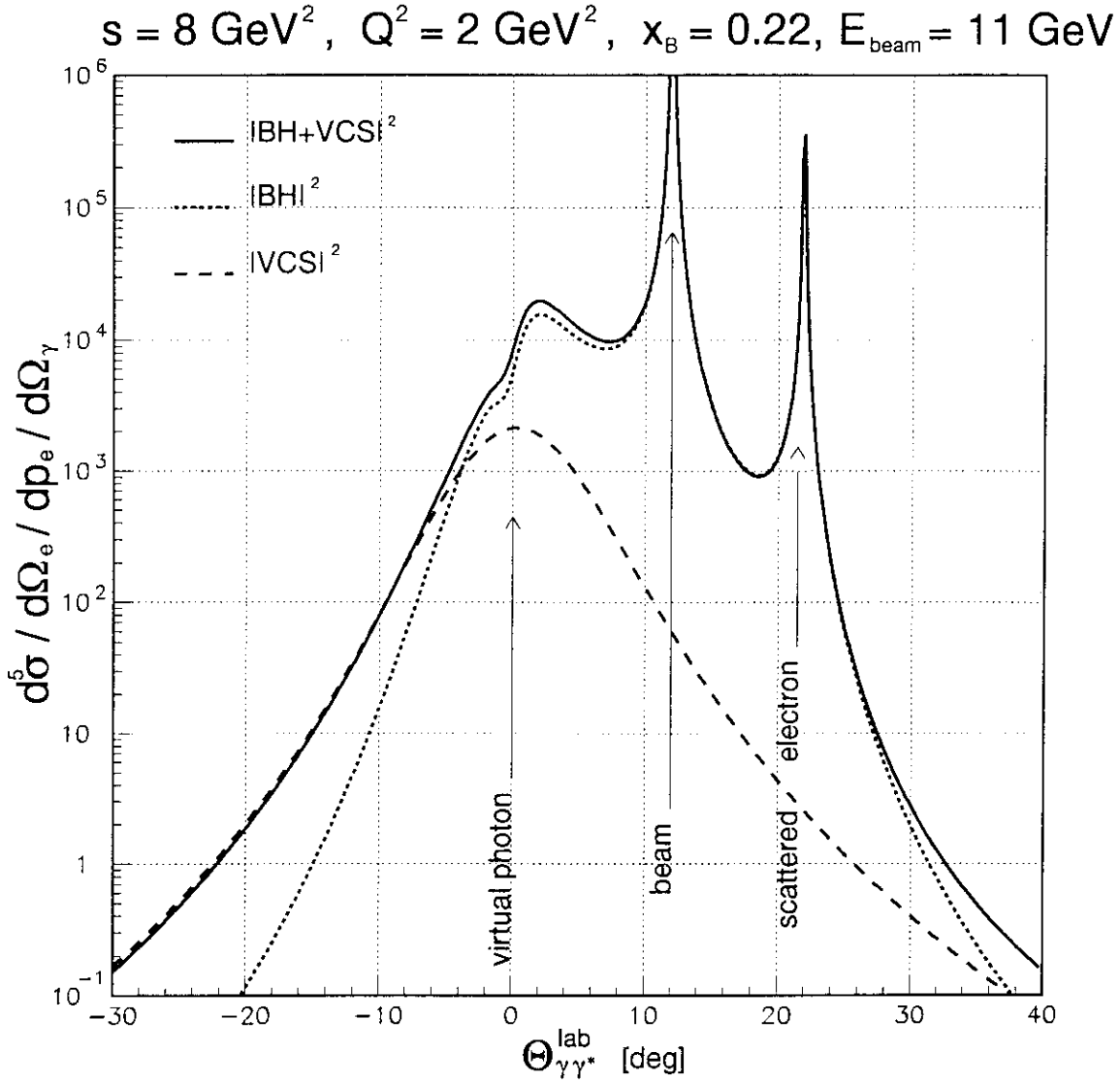

Figure 4: DVCS cross-section (target rest frame) calculated by using a model for the SPD's from P.A.M. Guichon and M. Vanderhaeghen. $\theta^{\rm lab}_{\gamma\gamma^*}$ is the laboratory polar angle between the final photon q' and the VCS virtual photon $q = k - k'$.

For experiments at luminosities $\geq 10^{37}$, the following equipment is required to isolate the exclusive channel:

- electron spectrometer with central momentum p_e=4–7 GeV and $\theta_e \geq 10°$,
- high performance photon calorimeter with solid angle ≈ 0.1 sr,
- recoil proton detector for $400 \leq p_p \leq 1$ GeV/c, covering ≈ 1 sr.

We want to emphasize that the detection of the recoil nucleon resolves the exclusive channel and does not penalize the counting rates.

Using a 11 GeV beam will enlarge the available kinematic range, as shown in Fig. 5 and 6. We could access a range in x from 0.1 to 0.5 and for values of Q^2 from 1 to 5 GeV^2 and s from 4 to 8 GeV^2. These values are in the scaling domain of deep inelastic scattering, where DVCS is also expected to scale. One must note that the main limitations for the kinematic range come from:

- The minimum angle between the photon calorimeter and the beam. The counting rate of the calorimeter increases dramatically as we go in the forward direction due to electromagnetic processes (moller scattering and photoproduction by real and quasi-real photons). Nevertheless, by using the sampling technique at 1 GHz as described in the 6 GeV proposal [25], angles as low as 10° can be achieved. The counting rates only increase by the logarithm of the incident energy and therefore will not be much different at 11 GeV than at 6 GeV.
- The other limitation comes from the minimum angle at which we can move the electron spectrometer. A spectrometer allowing measurements of 7 GeV electrons at ~10°-12° will be well suited to access the x_B range from 0.25 to 0.5. Halls A and C have plans to upgrade the current spectrometers and need to do so taking into considerations the DVCS requirements.

With a luminosity of 10^{37} and a electron acceptance $\Delta\Omega \cdot \Delta p_e/p_e > 5$ msr ·10%, each data point will require 200–400 hours of beam time to achieve a precision on the measurement of the helicity asymmetry of $\approx$ 10% of the predicted value.

5 Necessity of a positron beam

It is clear from the two first sections that measuring the imaginary part of the DVCS amplitude through a beam helicity asymmetry is not sufficient to obtain the full (x, ξ) dependence of the SPD's. Indeed, taking the imaginary part of the amplitude restrains the measurement to $x = \xi$, *i.e.* the border of the two regimes shown in Fig. 3. When $|x| > \xi$, the SPD's are essentially the ordinary parton distribution. When $|x| < \xi$ the SPD's are like meson wave fonctions. We want to thank P.A.M. Guichon to have stressed this important point [26]. We have to emphasize here that using a positron beam at Jefferson Lab would allow us to separately access the real part of the DVCS amplitude, therefore measuring a principal value integral over x of the SPD's, as explained in references [18] and [24]. Unlike the imaginary part, the real part depends on the SPD's also at $x \neq \xi$: the knowledge of the real part of the DVCS amplitude would give us the full (x, ξ) dependence of the SPD's. The measurement of the real part of the DVCS amplitude with a beam charge asymmetry, along with the measurement of the imaginary part of the DVCS amplitude with a beam helicity asymmetry would provide us with the complete complex amplitude.

Building a positron beam of few nano-amps is not a technological issue. Indeed, it was available 30 years ago in room temperature accelerators. CLAS in Hall B can accomodate this kind of beam currents and would be the natural place in which to perform a such an experiment. Nevertheless, beam of a few micro-amps are possible and some studies are starting a Jefferson Lab. If they succeed, then such a beam will allow us to create a full DVCS program at Jefferson Lab.

From an experimental point of view, Jefferson Lab takes advantage of the large Bethe-Heitler process. Indeed, the induced asymmetries (charge or helicity) are proportional to the full BH amplitude. This magnification and the high luminosity make Jefferson Lab a great place to study the SPD's.

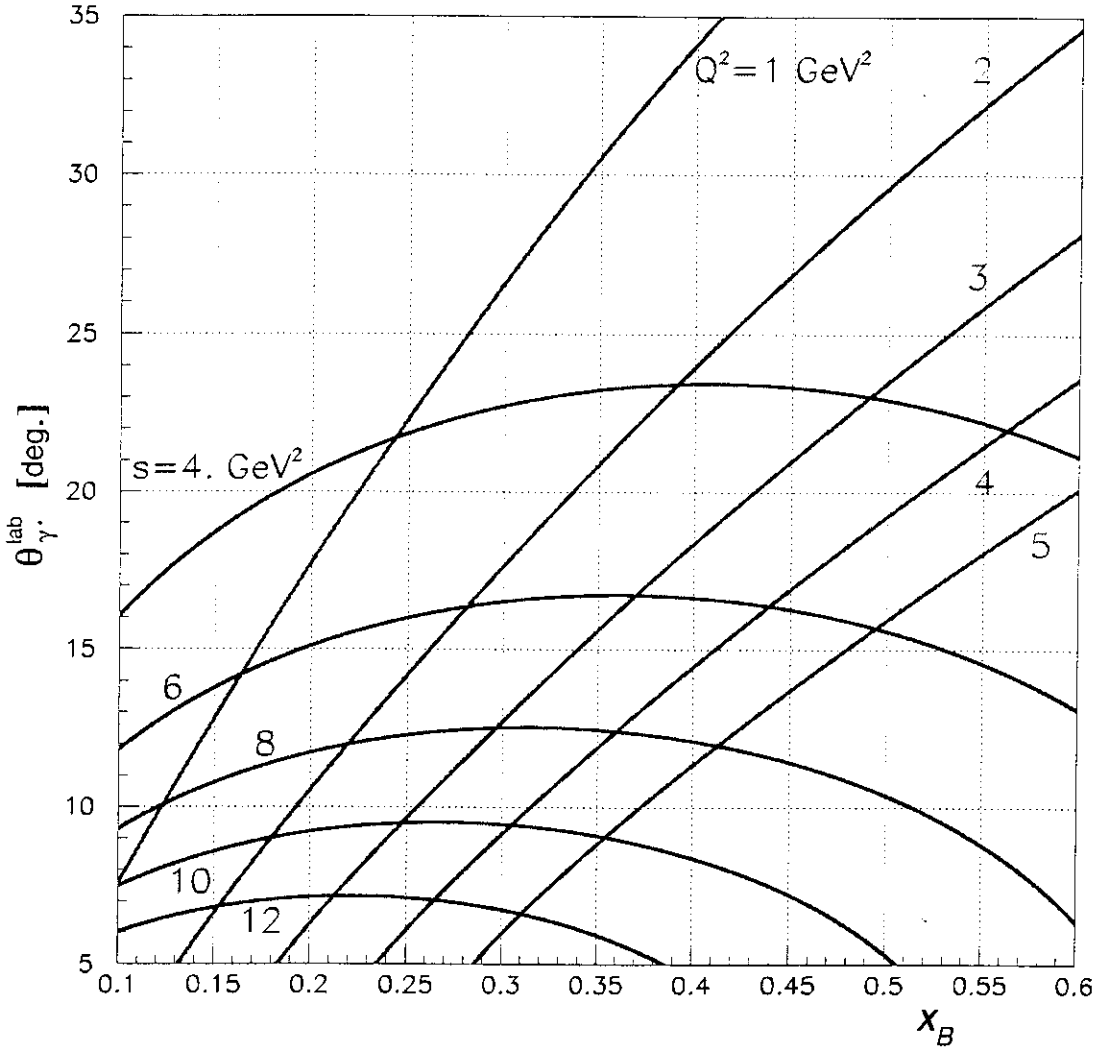

Figure 5: Angle of the virtual photon in the laboratory frame $\theta^{\rm lab}_{\gamma^*}$ versus x_B for an 11 GeV beam. Also plotted are the iso-$s = (q+p)^2$ and iso-Q^2 contours. Note that $\theta^{\rm lab}_{\gamma^*}$ is the angle where the photon calorimeter is located. Background in the calorimeter will limit measurements to $\theta^{\rm lab}_{\gamma^*} \geq 10^\circ$ at a luminosity of 10^{37}.

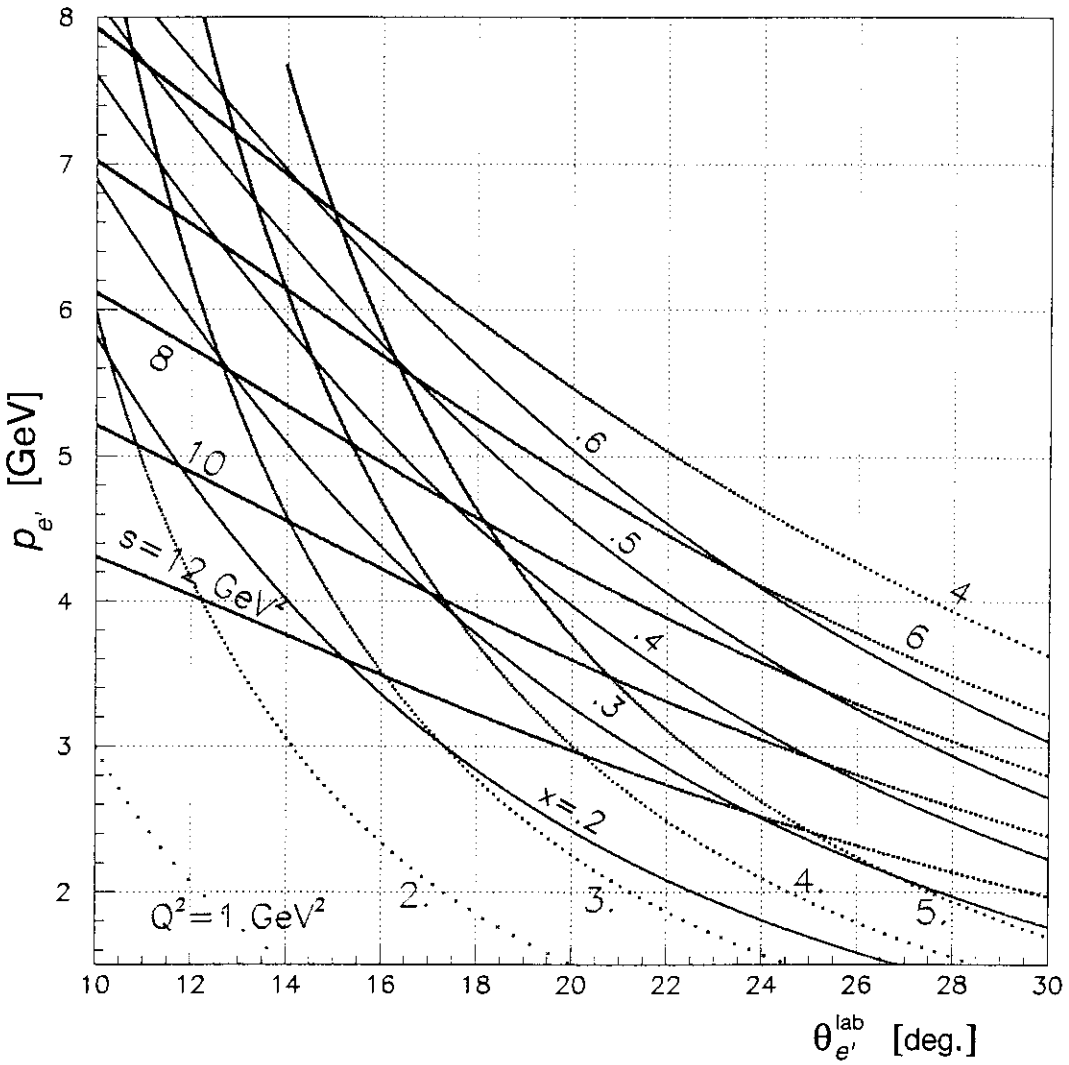

Figure 6: Incoming electron momentum p_e versus scattered electron angle $\theta_{e'}$ for an 11 GeV beam. Also plotted are the iso-$s = (q + p)^2$, iso-Q^2 and iso-x_B contours. For example, a kinematic point x_B=0.4, Q^2=4.0 GeV^2 at $E_{\rm beam}$=11 GeV requires p_e=5.7 GeV and $\theta_e = 14.5°$.

References

[1] R. Hofstadter, *Ann. Rev. Nucl. Sci.* **7**, 231 (1958)
M. Jones *et al.*, *Phys. Rev. Lett.* **84**, 1398 (2000).

[2] I. Passchier *et al.*, *Phys. Rev. Lett.* **82**, 4988 (1999)
D. Rohe *et al.*, *Phys. Rev. Lett.* **83**, 4257 (1999).

[3] K. Aniol *et al.*, *Phys. Rev. Lett.* **82**, 1096 (1999)
D. Spayde *et al.*, *Phys. Rev. Lett.* **84**, 1106 (2000).

[4] J. Friedman ad H. Kendall, *Ann. Rev. Nucl. Sci.* **22**, 203 (1972).

[5] K. Abe *et al.*, *Phys. Lett.* **B364**, 61 (1995)
K. Abe *et al.*, *Phys. Rev. Lett.* **79**, 26 (1997)
P. Anthony *et al.*, *Phys. Lett.* **B463**, 339 (1999).

[6] D. Adams *et al.*, *Phys. Lett.* **B396**, 338 (1997)
D. Adams *et al.*, *Phys. Rev.* **D56**, 5330 (1997).

[7] D. Drell and T. Yan, *Phys. Rev. Lett.* **25**, 316 (1970).

[8] J. Collins and A. Freund, *Phys. Rev.* **D59**, 074009 (1999).

[9] J. Collins, L. Frankfurt and M. Strikman, *Phys. Rev.* **D56**, 2982 (1997).

[10] X. Ji, *Phys. Rev. Lett* **78**, 610 (1997)
X. Ji, *Phys. Rev.* **D55**, 7114 (1997).

[11] D. Müller *et al.*, *Fort. Phys.* **42**, 101 (1994).

[12] A.V. Radyushkin, *Phys. Lett.* **B380**, 417 (1996)
A.V. Radyushkin, *Phys. Lett.* **B385**, 333 (1996).

[13] Yu. L. Dokshitser, *Sov. Phys.* JETP **46**, 641 (1977)
G. Altarelli and G. Parisi. *Nucl. Phys* **B126**, 298 (1977)
L.N. Lipatov, *Sov. J. Nucl. Phys.* **20**, 94 (1975).

[14] G.P. Lepage and S.J Brodsky, *Phys. Lett.*, **B87**, 359 (1979)
A.V. Efremov and A.V. Radyuskin, *Phys. Lett.*, **B94**, 245 (1980).

[15] A.V Belitsky *et al.*, *Phys. Lett.*, **B474**, 163 (2000).

[16] S.J. Brodsky, F. Close, J.F. Gunion, *Phys. Rev.* **D6**, 177 (1972).

[17] M. Diehl *et al.*, *Phys. Lett.* **B411**, 183 (1997).

[18] P.A.M. Guichon and M. Vanderhaeghen, *Prog. Part. Nucl. Phys* **41**, 125 (1998).

[19] I.V. Musatov and A.V. Radyushkin, *Phys. Rev.* **D61**, 74027 (2000).

[20] M. Penttinen, M.V. Polyakov and K. Goeke, **hep-ph/9909489**.

[21] M.V. Polyakov and C. Weiss, *Phys. Rev.* **D60**, 114017 (1999).

[22] L. Mankiewicz, G. Piller and T. Weigl, *Eur. Phys. J.* **C5**, 119 (1998)

[23] X. Ji *et al.*, *Phys. Rev.* **D56**, 5511 (1997).

[24] P.Y. Bertin, Y. Roblin and C.E. Hyde-Wright, Fizika **B8**, 207 (1999), **hep-ph/9910381**.

[25] Y. Roblin, F. Sabatié *et al*, Deeply Virtual Compton Scattering at 6 GeV, Jefferson Lab Hall A proposal P00-110. *http://www.jlab.org/~sabatie/dvcs/index.htm.*

[26] P.A.M. Guichon, private communication.